Published in final edited form as:
Int J Pharm. 2012 September 15; 434(1-2): 306–314. doi:10.1016/j.ijpharm.2012.05.028.

Co-administration strategy to enhance brain accumulation of vandetanib by modulating P-glycoprotein (P-gp/Abcb1) and breast cancer resistance protein (Bcrp1/Abcg2) mediated efflux with m-TOR inhibitors

Mukul Minocha, **Varun Khurana**, **Bin Qin**, **Dhananjay Pal**, and **Ashim K Mitra***
University of Missouri-Kansas City, School of Pharmacy, Division of Pharmaceutical Sciences

Abstract

The objectives of this study were (i) to characterize the interaction of vandetanib with P-glycoprotein (P-gp) and breast cancer resistance protein (Bcrp1) in vitro and in vivo (ii) to study the modulation of P-gp and BCRP mediated efflux of vandetanib with specific transport inhibitors and m-TOR inhibitors, everolimus and temsirolimus. Cellular accumulation and bi-directional transport studies in MDCKII cell monolayers were conducted to delineate the role of efflux transporters on disposition of vandetanib. Brain distribution studies were conducted in male FVB wild-type mice with vandetanib administered intravenously either alone or in the presence of specific inhibitors and m-TOR inhibitors. *In vitro* studies suggested that vandetanib is a high affinity substrate of Bcrp1 but is not transported by P-gp. Interestingly, in vivo brain distribution studies in FVB wild type mice indicated that vandetanib penetration into the brain is restricted by both Bcrp1 and P-gp mediated active efflux at the blood brain barrier (BBB). Co-administration of elacridar, a dual P-gp/BCRP inhibitor increased the brain to plasma concentration ratio of vandetanib upto 5 fold. Of the two m-TOR pathway inhibitors examined; everolimus showed potent effect on modulating vandetanib brain penetration whereas no significant affect on vandetanib brain uptake was observed following temsirolimus co-administration. This finding could be clinically relevant as everolimus can provide synergistic pharmacological effect in addition to primary role of vandetanib efflux modulation at BBB for the treatment of brain tumors.

Keywords

P-glycoprotein; breast cancer resistant protein; vandetanib; brain; efflux; pharmacokinetics

Introduction

ATP binding cassette (ABC) transporters P-glycoprotein (P-gp, ABCB1), multi-drug resistance associated protein (MRPs, ABCC) and breast cancer resistance protein (BCRP, ABCG2) are involved in translocation of a wide array of substrates across biological barriers. Apical localization of these membrane proteins on the gut, liver and kidney limits

***Corresponding author:** Ashim K. Mitra, Ph.D. Curators' Professor and Chairman Division of Pharmaceutical Sciences School of Pharmacy University of Missouri-Kansas City 2464 Charlotte Street Kansas City, MO 64108, USA Phone: 1-816-235-1615 Fax: 1-816-235-5190 mitraa@umkc.edu.

oral absorption and provides a mechanism for drug elimination (Leslie et al., 2005; Shugarts and Benet, 2009). The protective BBB also harbors these efflux proteins, which restrict the central nervous system (CNS) penetration of xenobiotics (Miller). Over expression of these efflux pumps in brain tumor tissues further compromises drug delivery (Gottesman et al., 2002; Loscher and Potschka, 2005). Many groups have previously reported the significance of ABC efflux pumps, especially P-gp and Bcrp1 in restricting the entry of numerous antitumor agents across BBB. Lapatinib, imatinib, gefitinib, erlotinib, and more recently axitinib and sunitnib have been reported to have restricted brain penetration due to P-gp and/or Bcrp1 mediated active efflux at the BBB (Polli et al., 2009; Agarwal et al., 2010; Breedveld et al., 2005; Kodaira et al., 2010; Poller et al., 2011; Tang et al., 2012)

Vandetanib (ZD6474), is an orally active inhibitor of vascular endothelial growth factor receptor (VEGFR), epidermal growth factor receptor (EGFR), and rearranged during transfection (RET) tyrosine kinases recently approved by the FDA for the treatment of metastatic medullary thyroid carcinoma (http://www.cancer.gov/cancertopics/druginfo/fda-vandetanib). In addition, phase III studies are currently ongoing for testing its efficacy against metastatic non small cell lung cancer (Heymach et al., 2008) (Clinicaltrials.gov, NCT00418886, NCT00312377 and NCT00404924). Furthermore, potent antitumor effects have been suggested in preclinical orthotopic brain tumor models (Sandstrom et al., 2004; Sandstrom et al., 2008) and several Phase I/II trials of vandetanib in newly diagnosed brain tumors are also ongoing (Broniscer et al., 2010; Drappatz et al., 2010). Adequate delivery of a chemotherapeutic agent to the invasive glioma cells located behind an intact BBB is a characteristic feature for optimal treatment of brain tumors. Numerous anti-cancer agents are subjected to active efflux leading to significantly reduced brain accumulation (Gottesman et al., 2002). Since clinical efficacy of vandetanib is currently under investigation for brain tumor treatment, it is relevant to know the interaction of vandetanib with these efflux proteins with respect to its brain penetration.

Given the fact that most of the anti-tumor agents are subject to efflux, a viable strategy to improve brain penetration is to inhibit the efflux activity at the BBB. Such inhibitors could significantly enhance the brain distribution of the substrate to therapeutically relevant concentrations in the target tumor tissue located behind an intact BBB. However, specific efflux modulators may cause systemic toxicity at doses required to modulate efflux activity and may not possess any inherent pharmacological action (Katragadda et al., 2005). Hence, a dual advantage could be achieved if the co-administered molecule has a synergistic pharmacological effect in addition to its primary role of efflux modulation. Apart from inhibiting VEGF mediated angiogenesis, there is emerging pre-clinical evidence suggesting pharmacological inactivation of m-TOR (mammalian target of rapamycin) pathway reduces neoplastic proliferation and brain tumor size (Galanis et al., 2005; Goudar et al., 2005). In human brain tumors, Akt/m-TOR pathway is activated in approximately 70% of the cases, in association with loss of PTEN and/or activation of EGFR and PDGFR tyrosine kinases (Hu et al., 2005). For this reason, everolimus and temsirolimus; two FDA approved m-TOR pathway inhibitors for the treatment of brain tumors, were chosen as clinically relevant efflux modulators for improving vandetanib brain delivery in this study.

Therefore one of the primary aim of this investigation was to determine whether vandetanib is a substrate for P-gp and/or BCRP and to delineate its effect on plasma and brain pharmacokinetics using appropriate cell culture and animal model. Further, we investigated if inhibition of the active efflux at the BBB could enhance the brain penetration of vandetanib using specific P-gp and BCRP inhibitors. In addition, from a clinical perspective, a combination therapy approach was evaluated to improve brain penetration of vandetanib upon co-administration of m-TOR inhibitors (everolimus and temsirolimus). We

hypothesize, if m-TOR inhibitors are able to modulate P-gp and BCRP activity at the BBB, a dual advantage could be realized for inclusion of these anticancer agents to vandetanib treatment regimen of brain tumor therapy. In addition to blocking both VEGF and m-TOR pathways; modulation of P-gp and BCRP mediated active efflux at the BBB could result in increased brain accumulation of vandetanib.

Materials and Methods

Chemicals

Vandetanib, everolimus, temsirolimus and pazopanib were purchased from LC Laboratories (Woburn, MA). [^{3}H]Digoxin and [^{3}H]Abacavir were purchased from PerkinElmer Life Sciences (Boston, MA) and Moravek Biochemicals (Brea, CA) respectively. Elacridar [GF120918, *N*-[4-[2-(6,7-dimethoxy-3,4-dihydro-1*H*-isoquinolin-2-yl)ethyl]-5-methoxy-9-oxo-10*H*-acridine-4-carboxamide]] was a generous gift from GlaxoSmithKline Ltd (Research Triangle,NC). Ko143, (a fumitremorgin C analog) was procured from Enzo Life Sciences (Plymouth Meeting, PA) and zosuquidar [LY335979] was kindly provided by Dr. Branimir Sikic at Stanford University, Kanisa Pharmaceuticals. Inc. (San Diego, CA). All other chemicals used were of high performance liquid chromatography grade and were obtained from fisher scientific.

In-vitro studies

Cell lines—Madin-Darby canine kidney (MDCKII) cells were used in all in vitro experiments. Parent MDCK-Wild-type (WT), MDR1 and Bcrp1-transfected cells were a gift from Drs. Piet Borst and Alfred H. Schinkel (The Netherlands Cancer Institute). Cells were cultured in Dulbecco's modified Eagle's medium, fortified with 10% heat inactivated fetal bovine serum (Atlanta Biologicals Inc., Lawrenceville, GA), HEPES, penicillin (100 μg/ml), streptomycin (100 μg/ml), and maintained at 37°C with 5% CO2 under humidifying conditions.

Cellular Accumulation Studies—Cellular accumulation studies were conducted in 12 well polyester plates (Coaster Corning, NY). MDCKII Cells were plated at a seeding density of 2×10^5 cells/well. The medium was changed every alternate day and the cells formed confluent monolayers in 3–4 days. On the day of the experiment, the medium was aspirated and replaced with 0.5ml of fresh medium containing 100nM vandetanib either in the absence or presence of specific inhibitors. For inhibition studies, the cells were treated with the inhibitors (1μM LY335979 for P-gp, 200 nM Ko143 for Bcrp1 and 5μM each of everolimus and temsirolimus) during both the preincubation (30min) and the accumulation periods (60min). After 1h of cellular accumulation the supernatant was aspirated and the cell monolayers were washed two times with ice cold phosphate buffer saline to arrest cellular accumulation. Finally, 0.5 ml of fresh DMEM medium was added to each well and the culture plates were stored at −80°C overnight to allow the cells to lyse. The following day, intracellular drug concentration was quantified by liquid chromatography tandem mass spectrometry (LC/MS-MS). The rate of cellular accumulation of the test drug was normalized to the protein content in each well. All stock solutions were prepared in DMSO such that final DMSO concentration in working solution did not exceed 0.5% (v/v).

Directional Transport Assays—Bi-directional transport experiments were carried out in 12-well Transwell inserts (Costar Corning, NY). Trans-epithelial transport of vandetanib was measured in two directions: apical-to-basolateral (A–B) and basolateral-to-apical (B–A). Experiment was initiated by addition of 5μM vandetanib in DMEM at the donor side. Samples (150 μl) were withdrawn from the receiver chamber at predetermined time points, i.e. 60, 120, 180 and 240 min and replaced with equal volume of fresh DMEM to maintain

sink conditions. In the inhibition studies, the inhibitors (1 μM LY335979, 200 nM Ko143, 5μM everolimus or 5μM temsirolimus) were added during the 1h preincubation step, as well as during the course of the experiment. Samples were stored in −80°C until further analysis by LC/MS-MS. Apparent permeability was obtained from the following equations:

$$P_{app} = (dm/dt) / A * C_d \quad (1)$$

Where, dM/dt is the rate of drug transport across cell monolayer, `A' represents the surface area available for transport and C_d is the initial drug concentration at donor chamber. The net efflux was assessed by calculating the efflux ratio as shown in Eq. 2. An efflux ratio greater than 1.5 indicates net efflux.

$$\text{Efflux Ratio} = \left(P_{app} B \rightarrow A\right) / \left(P_{app} A \rightarrow B\right) \quad (2)$$

Where, P_{app} B→A and P_{app} A→B indicates apparent drug permeability in the B to A and A to B direction, respectively.

P-gp and Bcrp1 inhibition by m-TOR inhibitors—Inhibition of P-gp and Bcrp1 by everolimus and temsirolimus was studied in MDCKII transfected cells using radiolabeled probe substrates, [^{3}H]digoxin for P-gp and [^{3}H]abacavir (ABC) for Bcrp1. Intracellular accumulation of these probe substrates in the presence of increasing concentrations (0.5–50μM) of everolimus and temsirolimus was measured in comparison to control. Wherever possible, dose-dependent inhibition data were fitted to a relationship described in the following equation.

$$Y = \min + \frac{\max - \min}{1 + 10^{(\text{LogIC}_{50} - x) \cdot H}} \quad (3)$$

Where, x denotes the logarithm of the concentration of the m-TOR inhibitors, Y is the cellular accumulation of the probe substrate, IC_{50} represents the inhibitor concentration where the efflux of the substrate is inhibited by 50% and H is the Hill constant. Y starts at a minimum value and then plateaus at a maximum (max) value (at high inhibitor concentration) resulting in a sigmoidal shape. Data were fitted to Eq. 3 with a transformed nonlinear regression curve analysis program (GraphPad Prism version 5.0, GraphPad Software Inc., San Diego, CA).

In vivo studies

Animals—Male FVB wild type mice were used as an animal model for in vivo experiments. All mice were between 8–11 weeks of age at the time of experiment. All animals were bought from Harlan laboratories, IN. Animals were used in accordance with the protocols approved by the University of Missouri-Kansas City (UMKC) Institutional Animal Care and Use Committee and housed in Laboratory Animal Care accredited facilities at UMKC. Animals were allowed to acclimatize for a minimum of 5 days before initiating the studies. Food and water were provided *ad libitum.*

Drug solutions—For intravenous administration vandetanib, elacridar (GF120918), Ko143, everolimus and temsirolimus were dissolved in 3:4:3, DMSO: propylene glycol: 0.9% saline v/v/v. Zosuquidar trihydrochloride (LY335979) was dissolved in 1:4, DMSO: 0.9% saline v/v.

Brain accumulation and plasma pharmacokinetics of vandetanib in FVB mice

All mice received vandetanib intravenously through tail vein injection at a dose of 5mg/kg. The study comprised of six different study groups:

Mice received an i.v dose of either vehicle, GF120918 (10mg/kg), LY335979 (25mg/kg), Ko143 (10mg/kg), everolimus (10mg/kg) or temsirolimus (10mg/kg) 30min before intravenous administration of vandetanib. In all study groups animals were euthanized using a CO_2 chamber at predetermined time points post dose (15, 30, 60, and 120 min, $n = 3$ for each time point). Blood was collected via cardiac puncture and transferred to heparin coated microcentrifuge tubes. Plasma was isolated from the blood by centrifugation at 10000 rpm for 7 min at 4°C. Whole brain was immediately removed, rinsed with ice-cold saline to remove extraneous blood and blot dried. All samples were stored at −80°C until further analysis by LC/MS-MS.

Analysis of vandetanib in mouse plasma and brain homogenate samples by LC/MS-MS

On the day of analysis, brain samples were weighed and homogenized in 3 volumes of 5% bovine serum albumin in water, using a tissue homogenizer (PRO Scientific Inc., oxford CT). Two separate standard curves were prepared for analyzing vandetanib from brain and plasma matrices. Fifty μl aliquots for plasma and 100ul aliquot of brain homogenate samples were spiked with 40ng of pazopanib (IS) and vortexed for 15 sec. The analytes were then extracted using 900ul of ice cold ethyl acetate and vortexed for 2 min. For efficient separation of the aqueous and organic layers, samples were centrifuged at 10,000 rpm for 7 min. After centrifugation, 700ul of the organic layer was collected and dried in vacuum. The residue was reconstituted in 100 μl of mobile phase and subsequently 5μl was injected onto the LC/MS-MS for analysis. The LC/MS-MS QTrap® API-3200 mass spectrometer, (Applied Biosystems, Foster City, CA, USA) equipped with Shimadzu 1100 Series quaternary pump (Shimadzu G1311A), vacuum degasser (Shimadzu G1379A) and autosampler (Prominence G1367A, Shimadzu scientific instruments., Columbia, MD, USA) was employed to analyze samples from cellular accumulation studies. HPLC separation was performed on an XTerra® MS C18 column 50 x 4.6mm, 5.0 μm (Waters, Milford, MA). The mobile phase consisted of 70% acetonitrile and 30% water with 0.1% formic acid, pumped at a flow rate of 0.25 ml/min. Analysis time was 4 min per run and both analytes eluted within 2–2.5 minutes. Multiple reactions monitoring (MRM) mode was utilized to detect the compounds of interest. The mass spectrometer was operated in the positive ion mode for detection. The precursor to product ions (Q1→Q3) selected for vandetanib and internal standard during quantitative optimization were (*m/z*) 475.0→112.0 and 438.1→357.2 respectively. The operational parameters for the tandem mass spectrum for each analyte were obtained after running them in quantitative optimization mode. The turbo ion spray setting and collision gas pressure were optimized (IS voltage: ± 5500 V, temperature: 350°C, nebulizer gas: 40 psi, curtain gas: 30 psi). The limits of quantification were found to be in the range of 3–5 ng/ml for vandetanib and IS. The extraction recovery from the medium, mouse plasma and brain homogenate ranged from 40–50%.

Pharmacokinetic analysis

All relevant pharmacokinetic parameters were calculated using noncompartmental analysis (Phoenix WinNonlin 6.0.1; Pharsight, Mountain View, CA) from concentration-time data in plasma and brain. The data were fitted to a noncompartmental model, with an i.v. bolus dose. Sparse sampling module was utilized for obtaining relevant pharmacokinetic parameters. The slopes of the terminal phase of concentration-time profiles were estimated by log-linear regression and the terminal rate constant (λz) was calculated from the slope. The terminal half-lives were calculated from the equation: $t_{1/2}$=0.693/ λz. The areas under

the concentration- time profiles for plasma (AUC_{plasma}) and brain (AUC_{brain}) from time 0 to t_{last} were calculated using the linear trapezoidal method.

Statistical analysis

All in vitro and in vivo experiments were conducted at least in triplicate. Results from in vivo experiments are expressed as mean ± standard error (S.E). All other results are expressed as mean ± standard deviation (S.D). Student t test was applied to determine statistical significance between two groups, with $p<0.05$ being considered statistically significant.

Results

Cellular uptake of vandetanib in MDCKII cells

Intracellular accumulation of vandetanib (100nM) was studied in MDCK parent (WT), MDR1 and Bcrp1 overexpressing cells. Vandetanib accumulation was approximately 50% lower in Bcrp1 overexpressing cells in comparison to that of WT cells, suggesting Bcrp1 is involved in efflux of vandetanib (Fig.1A). However, vandetanib accumulation in MDR1 overexpressing cells was not statistically different from WT cells, indicating P-gp might not be playing a role in its efflux (Fig.1B). Pre-treatment with 200nM Ko143, a specific Bcrp1 inhibitor, restored vandetanib cellular accumulation, such that there was no difference between Bcrp1 overexpressing and WT cellular accumulation (Fig1A).

Bi-directional transport of vandetanib across MDCKII cell monolayers

Transepithelial transport was carried out across MDCKII-WT, MDR1 and Bcrp1 overexpressing variants. Vandetanib (5μM) showed no directionality in transport across WT cells (Fig.2A). However, in Bcrp1 transfected cells the amount of vandetanib transport was much greater in B→A direction relative to WT cells (Fig.2C). The apparent permeability, P_{app}B→A of vandetanib was significantly greater than P_{app}A→B in MDKC-Bcrp1 cells, resulting in net efflux ratio (ER) of 7.5 (Table I). This directionality of efflux was completely inhibited in the presence of Ko143 (200nM, Fig.2D), such that the ER was 1. No significant difference was observed in the directional flux across MDR1 transfected cells (Fig.2B). This was in concordance with cellular uptake results, wherein, we did not see any significant difference in the cell accumulation between WT and MDR1 overexpressing cells.

P-gp and Bcrp1 inhibition by m-TOR inhibitors

To determine the potency of m-TOR inhibitors to inhibit P-gp and Bcrp1 functional activity, cellular accumulation experiments were conducted using probe substrates, ([^{3}H]digoxin for P-gp and [^{3}H]abacavir for BCRP) in the presence of increasing concentrations of everolimus and temsirolimus. Both everolimus and temsirolimus were equipotent in inhibiting P-gp mediated [^{3}H]digoxin efflux in MDCK-MDR1 cells (Fig.3). A modified log [dose]-response curve was applied to fit the data (equation 3) in order to obtain IC_{50} values. IC_{50} values for everolimus and temsirolimus for P-gp inhibition were 3.0μM and 3.5μM respectively. Similarly, in MDCK-Bcrp1 cells intracellular accumulation of [^{3}H]abacavir increased significantly in the presence of m-TOR inhibitors (Fig.4A and B). Due to the lack of attainment of a plateau phase and solubility issues, 3 concentrations (10, 25 and 50μM) each of everolimus and temsirolimus were tested.

Influence of m-TOR inhibitors on cellular accumulation and directional transport of vandetanib across MDCK-Bcrp1 cells

Since everolimus and temsirolimus appeared to be potent inhibitors of BCRP functional activity, we wanted to determine if co-administration of m-TOR inhibitors could restore the

cellular accumulation and directionality of flux in MDCK-Bcrp1 cells. Both everolimus and temsirolimus (5μM) enhanced vandetanib cellular accumulation to 220% relative to control (Fig1A). It is noteworthy, that the extent of increase was similar to that of Ko143, a specific BCRP inhibitor. A Similar trend was observed in the directional transport experiments; everolimus and temsirolimus abolished the directionality of vandetanib flux such that the ER after co-incubation was 1.4 and 1.1, respectively (Fig2 E&F, Table I).

Plasma and brain distribution of vandetanib in FVB mice in the presence of specific inhibitors

Brain and plasma concentration-time profiles were determined for intravenously administered vandetanib. Brain concentrations were significantly lower than the plasma concentration at all the selected time points (15, 30, 60 and 120min, Fig 5). To delineate whether P-gp and Bcrp1 were actively involved in efflux of vandetanib at BBB; LY335979 (25mg/kg) and Ko143 (10mg/kg) were dosed i.v., 30 min prior to vandetanib as specific inhibitors of P-gp and BCRP respectively. No significant difference in the plasma concentrations of vandetanib was observed at any of the selected time points after co-administration of specific inhibitors (Fig.6A). However, brain concentrations increased significantly in the later time point (120 min post dose, Fig 6B), suggesting both P-gp and Bcrp1 might be involved in restricting the brain penetration of vandetanib.

Effect of dual P-gp/BCRP inhibitor elacridar (GF120918) on plasma and brain pharmacokinetics of vandetanib in FVB mice

Pre-treatment with GF120918 (10mg/kg) did not have a statistically significant effect on plasma concentrations (Fig 6) but led to a dramatic increase in the brain concentrations at all selected time points relative to vehicle control (Fig 6B). Brain-plasma concentration ratio (C_b/C_p) values for vandetanib increased from 0.18 (control) to 1.03 sixty min post dose (Fig. 7) after GF120918 pre-treatment.

Non-compartmental analysis of vandetanib plasma and brain concentration time profiles yielded a terminal half life of 1.6h and 1.58h respectively of FVB wild type mice (Table II). No significant change in the plasma half life was seen after co-administration of GF120918; however, terminal half life in the brain was increased to 4.28h. Total body clearance was 9.36 and 10.33 ml/min/kg in the absence and presence of elacridar respectively. Volume of distribution was 1.41 l/kg upon co-administration of GF120918 as compared to that of 1.30 l/kg in control mice. The ratio of the $AUC_{(0\rightarrow tlast)brain}/AUC_{(0\rightarrow tlast)plasma}$ increased significantly (~3-fold) in the presence GF120918 to 0.642 as compared to 0.206.

Influence of m-TOR inhibitors on brain penetration of vandetanib in FVB mice

Everolimus and temsirolimus (10mg/kg each) were administered i.v. similar to GF120918 as dual inhibitors of P-gp and Bcrp1. Temsirolimus had no effect on plasma concentrations of vandetanib but everolimus significantly increased vandetanib plasma concentration at just one time point i.e. 120min post dose. Vandetanib brain concentrations increased significantly upon co-administration of everolimus at 60 and 120 min postdose with a subsequent increase in the brain to plasma concentration (C_b/C_p) values (~3-4-fold) (Fig.8A and B). Surprisingly, temsirolimus showed only a modest increase in the brain concentrations of vandetanib at only 120 min time point. However, this increase in the brain penetration was masked due to the corresponding elevation in plasma vandetanib levels, leading to insignificant increase in C_b/C_p ($p>0.05$)values in comparison to everolimus (Fig. 8A and B).

Discussion

Vandetanib is a potent VEGFR and EGFR receptor tyrosine kinase inhibitor (TKI) currently being evaluated in clinic for its application in brain tumor therapy (NCT00441142, clinicaltrials.gov). Active efflux via P-gp and BCRP at the BBB can be a rate limiting step for adequate delivery of chemotherapeutics to the target brain tumor cells located behind an intact BBB. Previously, one report attempted to demonstrate the interaction of vandetanib with these efflux proteins (Azzariti et al., 2010). However, lack of any in vivo studies failed to demonstrate the role of P-gp and BCRP in vandetanib brain disposition. In the present study we have tried to elucidate whether P-gp and BCRP can restrict brain penetration of vandetanib. Although, our data conclusively demonstrate that Bcrp1 plays a significant role in effluxing vandetanib in vitro, activity of both P-gp and Bcrp1 needs to be inhibited simultaneously in vivo to increase its brain accumulation. This is particularly interesting, as in the past, many research groups have demonstrated most of the TKIs that were shared P-gp/Bcrp1 substrates to be predominantly transported by P-gp with the only exception being sorafenib (Agarwal et al., 2011). Finally, from the clinical perspective, we show that co-administration of a clinically relevant efflux modulator, everolimus can effectively inhibit P-gp and Bcrp1 activity, leading to significantly increased vandetanib concentrations in the brain.

In-vitro studies conducted on MDCKII cell monolayers revealed that vandetanib is efficiently transported by Bcrp1; in contrast P-gp had negligible effect on the directionality of vandetanib transport (Fig.2 B–C). Restoration of vandetanib cellular accumulation upon co-incubation with specific transport inhibitors (Fig. 1A) across MDCKII-Bcrp1 cell monolayers, corroborated the predominant involvement of Bcrp1 mediated efflux in its disposition (Fig. 2D, Table. 1).

Influence of P-gp and Bcrp1 on transport of vandetanib across BBB was investigated by determining the brain-to-plasma concentration ratios (C_b/C_p) in the absence and presence of specific transport inhibitors in FVB wild type mice. Vandetanib brain concentrations were significantly lower than the corresponding plasma concentrations at all the selected time points (Fig.5). Pharmacokinetic parameters obtained from noncompartmental analysis suggested that vandetanib brain exposure (AUC_{brain}) was approximately 20% to that of systemic circulation ($AUC_{plasma)}$ (Table. II). Co-administration of either Ko143 (specific Bcrp1 inhibitor, 10mg/kg) or LY3335979 (specific P-gp inhibitor, 25mg/kg) did not have much impact on brain accumulation of vandetanib (Fig. 6B and Fig.7). Surprisingly, GF120918 (elacridar), a dual inhibitor of P-gp and Bcrp1 synergistically increased vandetanib C_b/C_p by ~5-fold (Fig.7). This suggests that even if vandetanib does not seem to be transported by P-gp in vitro, in vivo at the mouse BBB, both P-gp and Bcrp1 act in concert to limit the brain penetration of vandetanib. This finding is not uncommon as sorafenib and dantrolene in separate studies were found to be non substrates of P-gp in vitro, but both P-gp and Bcrp1 were involved in their efflux at mouse BBB (Agarwal et al., 2011). Similar results have also been obtained from our laboratory with pazopanib, a multitargeted TKI (*manuscript submitted for publication*). The authors suggested a possible explanation for this mechanism could be the difference in the relative expression and capacities of P-gp and Bcrp1 in the mouse brain. This theory may also be applied to vandetanib brain disposition. Previous reports suggest that P-gp is present in significantly greater amounts at the mRNA level as compared to murine Bcrp1 at the mouse brain (Warren et al., 2009). In a similar fashion, Kamiie, et.al reported approx.5- fold higher levels of P-gp compared to Bcrp1 at the mouse BBB using a LC-MS assay (Kamiie et al., 2008). Hence, for a dual substrate even if the affinity is high for Bcrp1, P-gp might compensate for the loss in affinity by its higher capacity for efflux. In other words, only simultaneous inhibition of P-gp and Bcrp1 could enhance cerebral accumulation of vandetanib.

Inhibition of efflux is a viable strategy in overcoming drug resistance in chemotherapy (Breedveld et al., 2006). Specific efflux modulators can enhance brain penetration of substrate drug molecules. Although much of the data regarding efflux modulation are available from pre-clinical studies, first clinical study was reported by Sasongko et.al wherein, enhanced brain penetration of verapamil; a probe P-gp substrate, was demonstrated using PET imaging upon co-administration of a potent and specific P-gp inhibitor; cyclosporine A (Sasongko et al., 2005). In another report, Wagner and co-workers published similar findings employing a similar approach upon co-administration of tariquidar as a P-gp inhibitor using PET imaging (Wagner et al., 2009). Many attempts have been made to overcome multidrug resistance in oncology leading to development of numerous transport inhibitors, thus far with limited clinical success (Tamaki et al., 2011). Although potent, specific efflux modulators might not be clinically relevant primarily because of non-inherent pharmacological action and potential for toxicity. Hence, a dual advantage could be realized if the selected inhibitor has a therapeutic implication to be added in the existing treatment regimen. Since inhibition of m-TOR pathway has been indicated as a potential strategy for brain tumor therapy (Goudar et al., 2005), we selected everolimus and temsirolimus as potential candidates for modulating P-gp and BCRP mediated efflux of vandetanib. Everolimus and temsirolimus have been used as monotherapy in treatment of brain metastasis and now are under investigation for treatment of several solid tumors (Galanis et al., 2005). Both everolimus and temsirolimus have been suggested to be transported by P-gp (Crowe and Lemaire, 1998), but their P-gp and BCRP inhibitory potential has not been elucidated thoroughly. As a secondary aim of this investigation, we studied P-gp and BCRP inhibitory potency of everolimus and temsirolimus using probe radiolabeled substrates. Both drugs increased the cellular accumulation of [^{3}H]digoxin, (substrate for P-gp) and [^{3}H]abacavir (substrate of Bcrp1) in a concentration dependent manner (Figs 3&4). Interestingly, both drugs were equipotent in inhibiting P-gp and BCRP mediated efflux, suggesting a similar inhibitory potency towards these efflux proteins. As expected, co-incubation of everolimus and temsirolimus, enhanced vandetanib cellular accumulation and reduced its efflux ratio to near unity; similar to that of a Ko143 (Fig. 1A and Fig.2D–F).

The finding that only GF120918 synergistically increased vandetanib brain distribution was particularly interesting as in vitro experiments also suggested both m-TOR inhibitors to be dual P-gp and BCRP inhibitors. Hence, we further explored if simultaneous inhibition of P-gp and BCRP by m-TOR inhibitors at the mouse BBB could also increase the brain distribution of vandetanib. Everolimus (10mg/kg) similar to GF120918, significantly increased (3–4-fold) the brain concentration of vandetanib 60 and 120 min postdose (Fig.8A and B); whereas temsirolimus (10mg/kg) demonstrated a statistically non significant increase ($p>0.05$) in brain concentration only at 120 min time point. The fact that everolimus had a more pronounced effect compared to temsirolimus was intriguing as both the drugs showed similar affinity and potency in inhibiting P-gp and BCRP mediated efflux in vitro. This discrepancy could be explained in part by the differences in the substrate binding sites for temsirolimus and vandetanib. It has been shown previously that multiple binding sites do exist on transport proteins P-gp and BCRP (Ambudkar et al., 2006; Giri et al., 2009). The results obtained from the current study suggest that digoxin, a prototypical P-gp substrate (used in vitro) binds to a similar site where its transport by P-gp is completely inhibited by temsirolimus. In contrast, vandetanib may bind to P-gp at a site distinct from the binding site of digoxin, where temsirolimus is able to only partially inhibit the interaction with P-gp. As we have seen that only simultaneous inhibition of P-gp/Bcrp1 could increase vandetanib brain accumulation, this could hold true only for everolimus but not for temsirolimus at the mouse BBB.

In light of much disappointing results obtained from the clinical studies in treatment of primary brain tumors after monotherapy, co-administration strategy might be a useful tool.

This multimodal approach will not only target multiple angiogenic pathways but may also increase the permeability of substrate drug molecules by inhibiting P-gp and Bcrp1 mediated efflux resulting in enhanced pharmacodynamic response in brain tumor therapy. Previously, many research groups have suggested co-administration of GF120918 for improving brain penetration of several molecularly targeted agents (Bihorel et al., 2007; Lagas et al., 2009). However, clinical application of GF120918 is still not yet established. Our results show that everolimus, although not as potent as GF120918, could modulate vandetanib brain accumulation to a significant extent. Since, everolimus is already approved by the FDA; this proof of concept study warrants further clinical investigation for employing everolimus as an efflux modulator in adjunct to vandetanib monotherapy for the treatment of recurrent brain tumors.

References

Agarwal S, Sane R, Gallardo JL, Ohlfest JR, Elmquist WF. Distribution of gefitinib to the brain is limited by P-glycoprotein (ABCB1) and breast cancer resistance protein (ABCG2)-mediated active efflux. J Pharmacol Exp Ther. 2010; 334:147–155. [PubMed: 20421331]

Agarwal S, Sane R, Ohlfest JR, Elmquist WF. The role of the breast cancer resistance protein (ABCG2) in the distribution of sorafenib to the brain. J Pharmacol Exp Ther. 2010; 336:223–233. [PubMed: 20952483]

Ambudkar SV, Kim IW, Sauna ZE. The power of the pump: mechanisms of action of P-glycoprotein (ABCB1). Eur J Pharm Sci. 2006; 27:392–400. [PubMed: 16352426]

Azzariti A, Porcelli L, Simone GM, Quatrale AE, Colabufo NA, Berardi F, Perrone R, Zucchetti M, D'Incalci M, Xu JM, Paradiso A. Tyrosine kinase inhibitors and multidrug resistance proteins: interactions and biological consequences. Cancer Chemother Pharmacol. 2010; 65:335–346. [PubMed: 19495754]

Bihorel S, Camenisch G, Lemaire M, Scherrmann JM. Modulation of the brain distribution of imatinib and its metabolites in mice by valspodar, zosuquidar and elacridar. Pharm Res. 2007; 24:1720–1728. [PubMed: 17380257]

Breedveld P, Beijnen JH, Schellens JH. Use of P-glycoprotein and BCRP inhibitors to improve oral bioavailability and CNS penetration of anticancer drugs. Trends Pharmacol Sci. 2006; 27:17–24. [PubMed: 16337012]

Breedveld P, Pluim D, Cipriani G, Wielinga P, van Tellingen O, Schinkel AH, Schellens JH. The effect of Bcrp1 (Abcg2) on the in vivo pharmacokinetics and brain penetration of imatinib mesylate (Gleevec): implications for the use of breast cancer resistance protein and P-glycoprotein inhibitors to enable the brain penetration of imatinib in patients. Cancer Res. 2005; 65:2577–2582. [PubMed: 15805252]

Broniscer A, Baker JN, Tagen M, Onar-Thomas A, Gilbertson RJ, Davidoff AM, Pai Panandiker AS, Leung W, Chin TK, Stewart CF, Kocak M, Rowland C, Merchant TE, Kaste SC, Gajjar A. Phase I study of vandetanib during and after radiotherapy in children with diffuse intrinsic pontine glioma. J Clin Oncol. 28:4762–4768. [PubMed: 20921456]

Crowe A, Lemaire M. In vitro and in situ absorption of SDZ-RAD using a human intestinal cell line (Caco-2) and a single pass perfusion model in rats: comparison with rapamycin. Pharm Res. 1998; 15:1666–1672. [PubMed: 9833985]

Drappatz J, Norden AD, Wong ET, Doherty LM, Lafrankie DC, Ciampa A, Kesari S, Sceppa C, Gerard M, Phan P, Schiff D, Batchelor TT, Ligon KL, Young G, Muzikansky A, Weiss SE, Wen PY. Phase I study of vandetanib with radiotherapy and temozolomide for newly diagnosed glioblastoma. Int J Radiat Oncol Biol Phys. 2010; 78:85–90. [PubMed: 20137866]

Galanis E, Buckner JC, Maurer MJ, Kreisberg JI, Ballman K, Boni J, Peralba JM, Jenkins RB, Dakhil SR, Morton RF, Jaeckle KA, Scheithauer BW, Dancey J, Hidalgo M, Walsh DJ. Phase II trial of temsirolimus (CCI-779) in recurrent glioblastoma multiforme: a North Central Cancer Treatment Group Study. J Clin Oncol. 2005; 23:5294–5304. [PubMed: 15998902]

Giri N, Agarwal S, Shaik N, Pan G, Chen Y, Elmquist WF. Substrate-dependent breast cancer resistance protein (Bcrp1/Abcg2)-mediated interactions: consideration of multiple binding sites in in vitro assay design. Drug Metab Dispos. 2009; 37:560–570. [PubMed: 19056916]

Gottesman MM, Fojo T, Bates SE. Multidrug resistance in cancer: role of ATP-dependent transporters. Nat Rev Cancer. 2002; 2:48–58. [PubMed: 11902585]

Goudar RK, Shi Q, Hjelmeland MD, Keir ST, McLendon RE, Wikstrand CJ, Reese ED, Conrad CA, Traxler P, Lane HA, Reardon DA, Cavenee WK, Wang XF, Bigner DD, Friedman HS, Rich JN. Combination therapy of inhibitors of epidermal growth factor receptor/vascular endothelial growth factor receptor 2 (AEE788) and the mammalian target of rapamycin (RAD001) offers improved glioblastoma tumor growth inhibition. Mol Cancer Ther. 2005; 4:101–112. [PubMed: 15657358]

Heymach JV, Paz-Ares L, De Braud F, Sebastian M, Stewart DJ, Eberhardt WE, Ranade AA, Cohen G, Trigo JM, Sandler AB, Bonomi PD, Herbst RS, Krebs AD, Vasselli J, Johnson BE. Randomized phase II study of vandetanib alone or with paclitaxel and carboplatin as first-line treatment for advanced non-small-cell lung cancer. J Clin Oncol. 2008; 26:5407–5415. [PubMed: 18936474]

Hu X, Pandolfi PP, Li Y, Koutcher JA, Rosenblum M, Holland EC. mTOR promotes survival and astrocytic characteristics induced by Pten/AKT signaling in glioblastoma. Neoplasia. 2005; 7:356–368. [PubMed: 15967113]

Kamiie J, Ohtsuki S, Iwase R, Ohmine K, Katsukura Y, Yanai K, Sekine Y, Uchida Y, Ito S, Terasaki T. Quantitative atlas of membrane transporter proteins: development and application of a highly sensitive simultaneous LC/MS/MS method combined with novel in-silico peptide selection criteria. Pharm Res. 2008; 25:1469–1483. [PubMed: 18219561]

Katragadda S, Budda B, Anand BS, Mitra AK. Role of efflux pumps and metabolising enzymes in drug delivery. Expert Opin Drug Deliv. 2005; 2:683–705. [PubMed: 16296794]

Kodaira H, Kusuhara H, Ushiki J, Fuse E, Sugiyama Y. Kinetic analysis of the cooperation of P-glycoprotein (P-gp/Abcb1) and breast cancer resistance protein (Bcrp/Abcg2) in limiting the brain and testis penetration of erlotinib, flavopiridol, and mitoxantrone. J Pharmacol Exp Ther. 2010; 333:788–796. [PubMed: 20304939]

Lagas JS, van Waterschoot RA, van Tilburg VA, Hillebrand MJ, Lankheet N, Rosing H, Beijnen JH, Schinkel AH. Brain accumulation of dasatinib is restricted by P-glycoprotein (ABCB1) and breast cancer resistance protein (ABCG2) and can be enhanced by elacridar treatment. Clin Cancer Res. 2009; 15:2344–2351. [PubMed: 19276246]

Leslie EM, Deeley RG, Cole SP. Multidrug resistance proteins: role of P-glycoprotein, MRP1, MRP2, and BCRP (ABCG2) in tissue defense. Toxicol Appl Pharmacol. 2005; 204:216–237. [PubMed: 15845415]

Loscher W, Potschka H. Drug resistance in brain diseases and the role of drug efflux transporters. Nat Rev Neurosci. 2005; 6:591–602. [PubMed: 16025095]

Miller DS. Regulation of P-glycoprotein and other ABC drug transporters at the blood-brain barrier. Trends Pharmacol Sci. 31:246–254. [PubMed: 20417575]

Poller B, Iusuf D, Sparidans RW, Wagenaar E, Beijnen JH, Schinkel AH. Differential Impact of P-Glycoprotein (ABCB1) and Breast Cancer Resistance Protein (ABCG2) on Axitinib Brain Accumulation and Oral Plasma Pharmacokinetics. Drug Metab Dispos. 2011; 39:729–735. [PubMed: 21282407]

Polli JW, Olson KL, Chism JP, John-Williams LS, Yeager RL, Woodard SM, Otto V, Castellino S, Demby VE. An unexpected synergist role of P-glycoprotein and breast cancer resistance protein on the central nervous system penetration of the tyrosine kinase inhibitor lapatinib (N-{3-chloro-4-[(3-fluorobenzyl)oxy]phenyl}-6-[5-({[2-(methylsulfonyl)ethyl]amino }methyl)-2-furyl]-4-quinazolinamine; GW572016). Drug Metab Dispos. 2009; 37:439–42. [PubMed: 19056914]

Sandstrom M, Johansson M, Andersson U, Bergh A, Bergenheim AT, Henriksson R. The tyrosine kinase inhibitor ZD6474 inhibits tumour growth in an intracerebral rat glioma model. Br J Cancer. 2004; 91:1174–1180. [PubMed: 15305185]

Sandstrom M, Johansson M, Bergstrom P, Bergenheim AT, Henriksson R. Effects of the VEGFR inhibitor ZD6474 in combination with radiotherapy and temozolomide in an orthotopic glioma model. J Neurooncol. 2008; 88:1–9. [PubMed: 18228115]

Sasongko L, Link JM, Muzi M, Mankoff DA, Yang X, Collier AC, Shoner SC, Unadkat JD. Imaging P-glycoprotein transport activity at the human blood-brain barrier with positron emission tomography. Clin Pharmacol Ther. 2005; 77:503–514. [PubMed: 15961982]

Shugarts S, Benet LZ. The role of transporters in the pharmacokinetics of orally administered drugs. Pharm Res. 2009; 26:2039–2054. [PubMed: 19568696]

Tamaki A, Ierano C, Szakacs G, Robey RW, Bates SE. The controversial role of ABC transporters in clinical oncology. Essays Biochem. 2011; 7:209–232. [PubMed: 21967059]

Tang SC, Lagas JS, Lankheet NA, Poller B, Hillebrand MJ, Rosing H, Beijnen JH, Schinkel AH. Brain accumulation of sunitinib is restricted by P-glycoprotein (ABCB1) and breast cancer resistance protein (ABCG2) and can be enhanced by oral elacridar and sunitinib coadministration. Int J Cancer. 2012

Wagner CC, Bauer M, Karch R, Feurstein T, Kopp S, Chiba P, Kletter K, Löscher W, Müller M, Zeitlinger M, Langer O. A pilot study to assess the efficacy of tariquidar to inhibit P-glycoprotein at the human blood-brain barrier with (R)-11C-verapamil and PET. J Nucl Med. 2009; 50:1954–1961. [PubMed: 19910428]

Warren MS, Zerangue N, Woodford K, Roberts LM, Tate EH, Feng B, Li C, Feuerstein TJ, Gibbs J, Smith B, de Morais SM, Dower WJ, Koller KJ. Comparative gene expression profiles of ABC transporters in brain microvessel endothelial cells and brain in five species including human. Pharmacol Res. 2009; 59:404–413. [PubMed: 19429473]

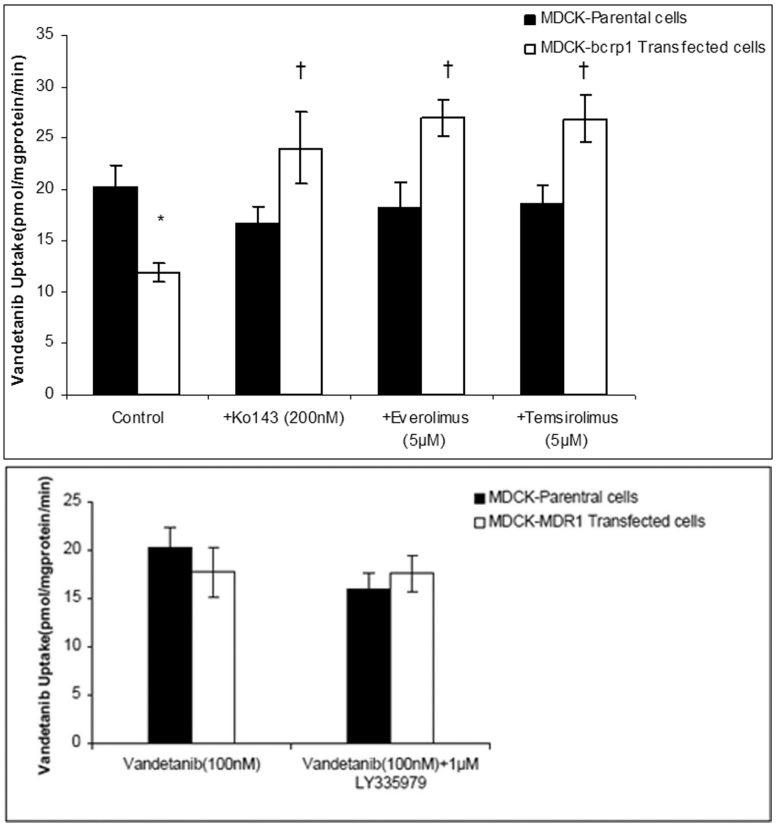

Fig.1.

Cellular accumulation of vandetanib (100nM) in MDCKII cells. A. Cellular accumulation of vandetanib in Bcrp1 Transfected cells (open bars) was approximately 50% less in comparison to that of parent WT cells (black bars). Pre-incubation with Ko143 (200nM), specific Bcrp1 inhibitor, restored the cell accumulation. Also, everolimus and temsirolimus (5μM each) effectively abolished the difference in cell uptake by inhibition of Bcrp1. B. Cellular accumulation in MDRI transfected cells was not statistically significant relative to parent WT cells. Specific P-gp inhibitor, LY335979 did not have any effect on vandetanib cell accumulation. Results are expressed as Mean±S.D. n=4. (* represents $p<0.05$ from parent WT control cells, whereas † represents $p<0.05$ from Bcrp1 control cells).

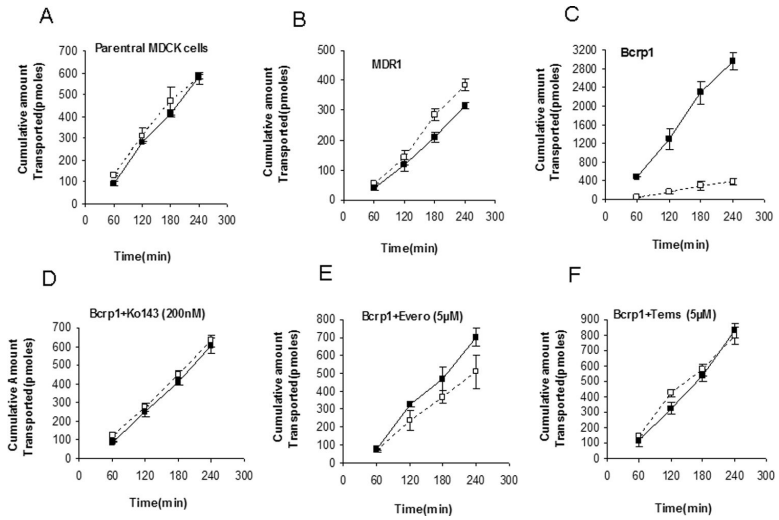

Fig.2.

Transepithelial transport of vandetanib (5μM) across MDCKII cell monolayers. Bi-directional transport was carried out in MDCKII parent (A), MDR1 (B) and murine Bcrp1(C) transfected cell monolayers. Significant directionality of transport was observed in Bcrp1 transduced MDCKII cells, this net flux was abolished upon preincubating 200nM Ko143 (D), a specific Bcrp1 inhibitor. Also, everolimus and temsirolimus (E and F) were both equally potent (at 5μM), to eliminate the directionality of vandetanib flux. (

); translocation from apical-to-basolateral chamber, (

), translocation from basolateral-to-apical chamber. Results are expressed as Mean±S.D. n=3 wells.

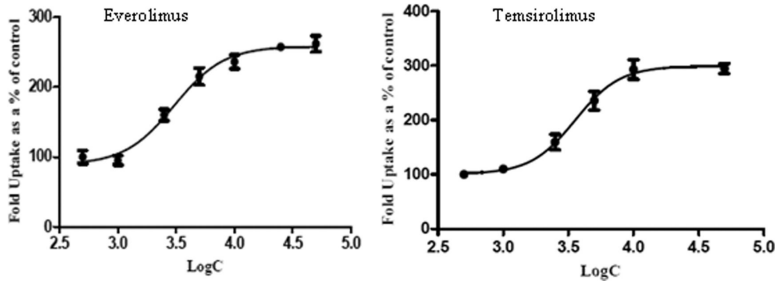

Fig.3.

Inhibition of P-gp by m-TOR inhibitors. Intracellular accumulation of P-gp substrate [^{3}H]digoxin in the presence of increasing concentrations of everolimus and temsirolimus. Values are expressed as (the percentage of control) Mean±S.D., n=3.

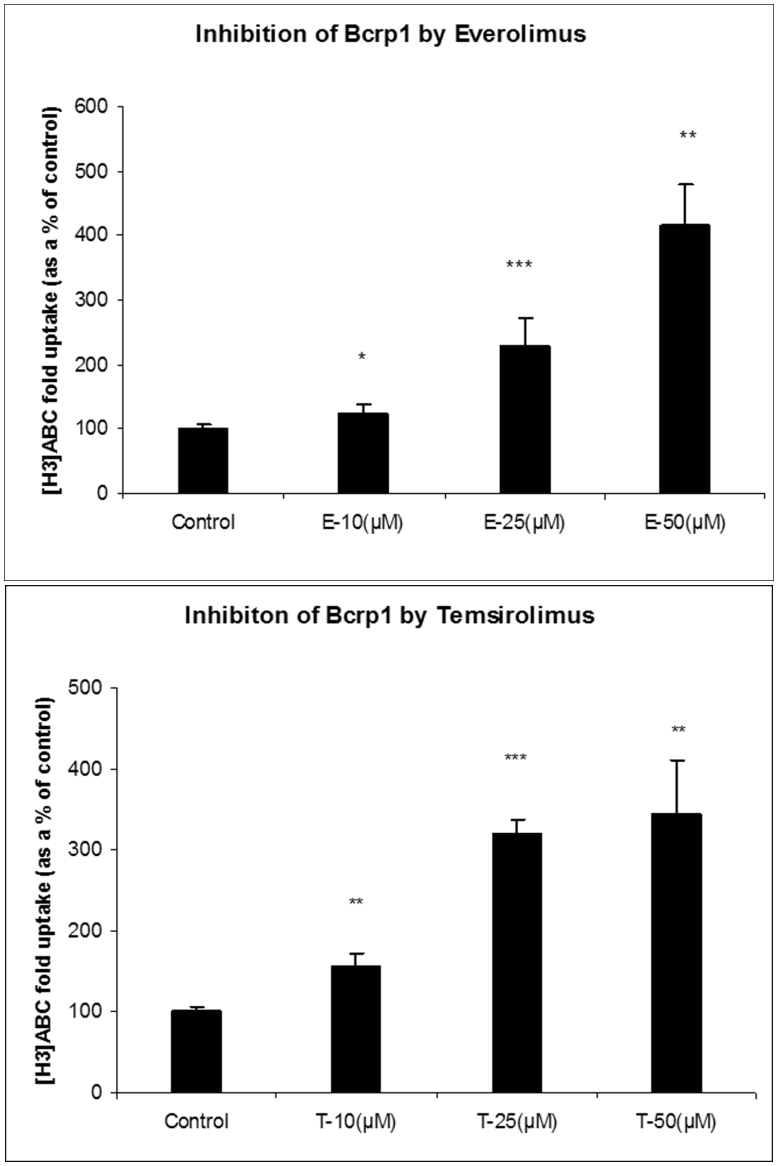

Fig.4.

Inhibition of Bcrp1 by m-TOR inhibitors: Intracellular accumulation of Bcrp1 substrate [^{3}H]abacavir (ABC) in the absence and presence of increasing concentrations of everolimus (A) and temsirolimus (B). Values are expressed as (the percentage of control) Mean±S.D., n=3. (*, ** and *** represents $p<0.05$, $p<0.01$ and $p<0.001$ respectively).

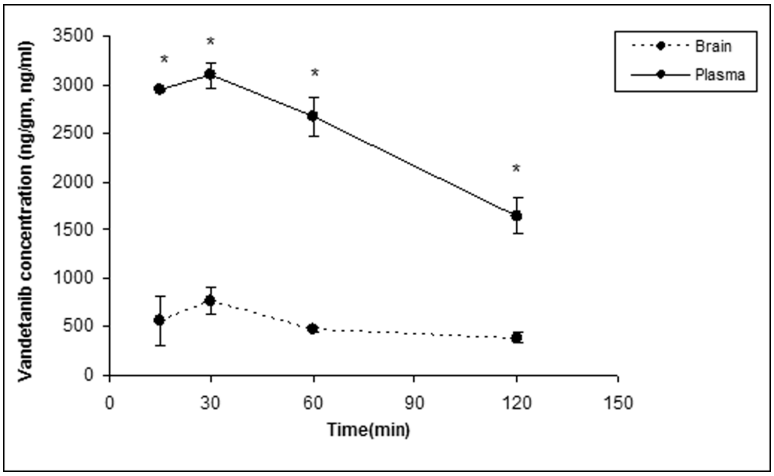

Fig. 5.

Vandetanib plasma and brain concentration-time profile. A single intravenous dose of vandetanib (5mg/kg) was administered through tail vein in FVB-wild type mice. Results are expressed as Mean±S.E., n=3. (* represents $p<0.05$).

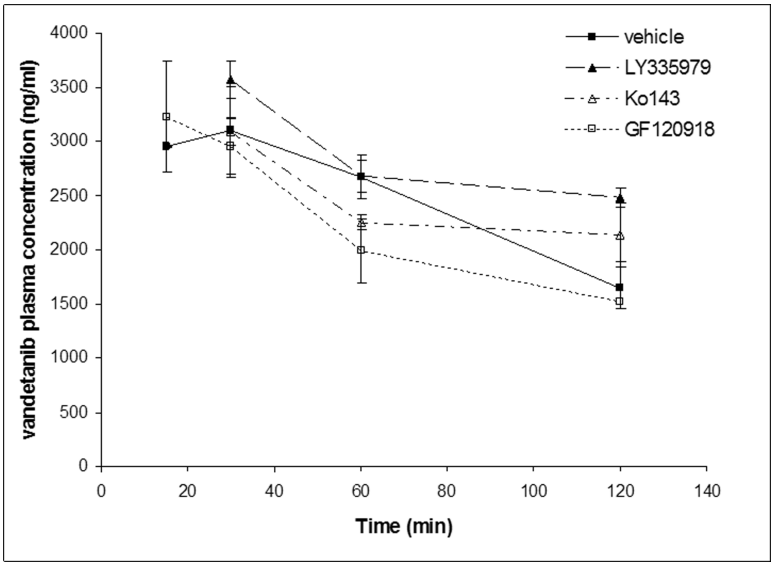

Fig.6A.

Vandetanib plasma concentration-time profile in the absence and presence of specific P-gp (LY335979, 25mg/kg), Bcrp1 (Ko143, 10mg/kg) and dual P-gp/Bcrp1 inhibitor (GF120918, 10mg/kg) administered i.v, 30 min prior to a single intravenous dose of vandetanib (5mg/kg) through tail vein in FVB-wild type mice. Results are expressed as Mean±S.E., n=3.

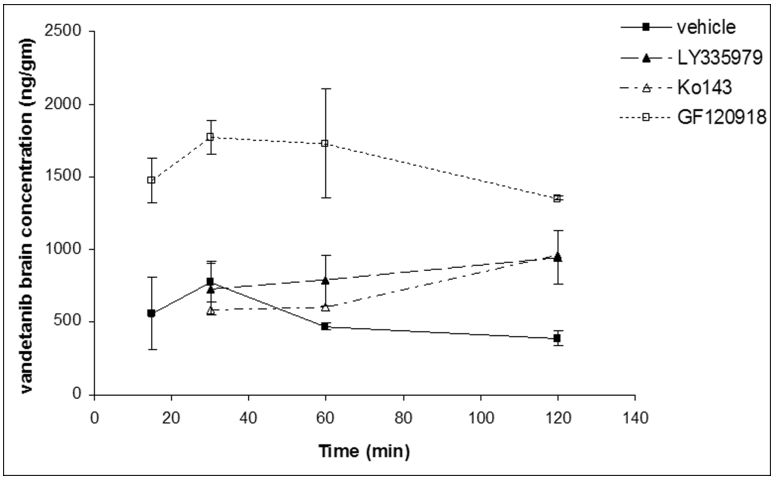

Fig.6B.

Vandetanib brain concentration-time profile in the absence and presence of specific P-gp (LY335979, 25mg/kg), Bcrp1 (Ko143, 10mg/kg) and dual P-gp/Bcrp1 inhibitor (GF120918, 10mg/kg) administered i.v, 30 min prior to a single intravenous dose of vandetanib (5mg/kg) through tail vein in FVB-wild type mice. Results are expressed as Mean±S.E., n=3.

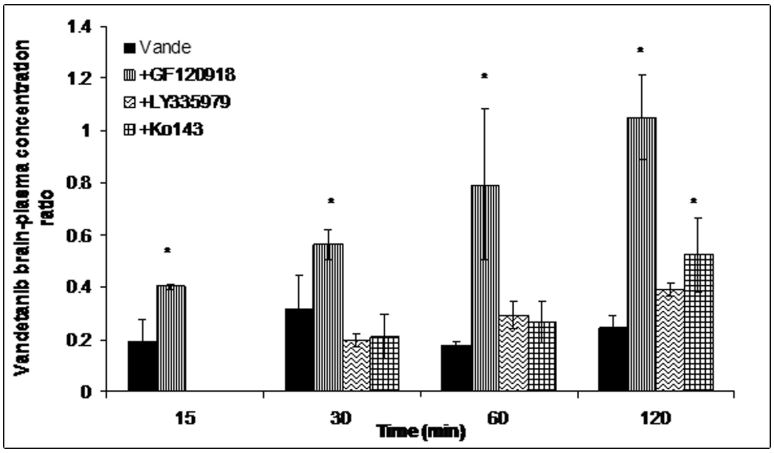

Fig.7.

Brain-to-plasma concentration ratios of vandetanib either alone or in the presence of specific inhibitors at 15, 30, 60 and 120min after an intravenous dose of 5mg/kg in FVB wild type mice. Results are expressed as Mean±S.E., n=3. (* represents $p<0.05$).

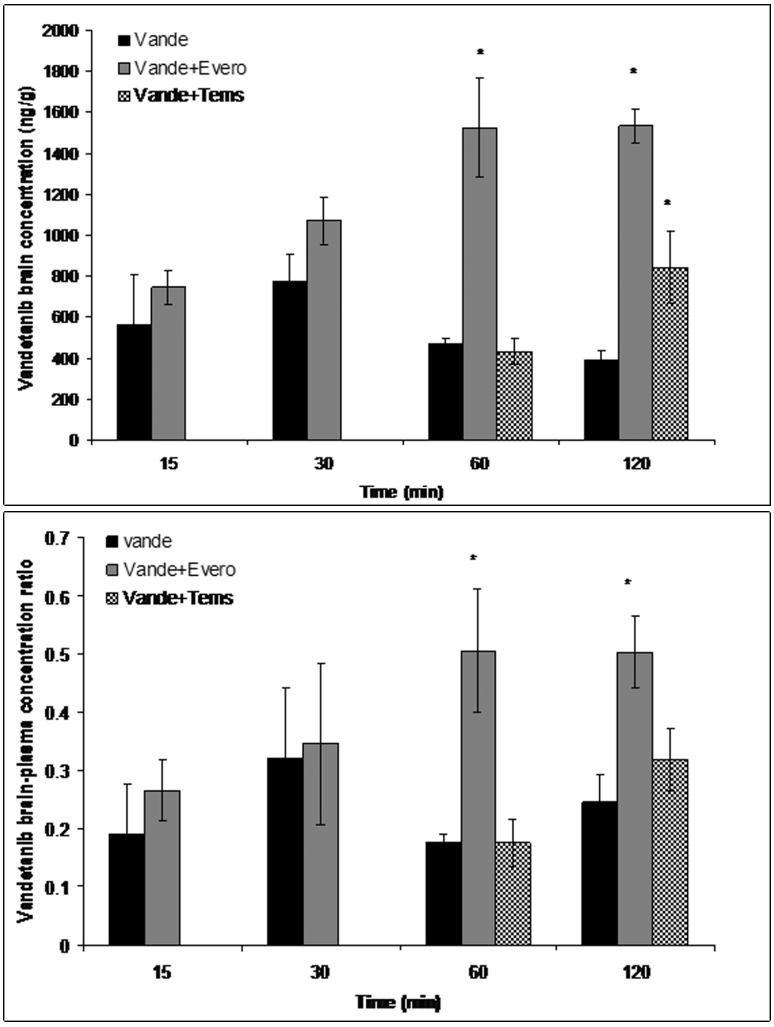

Fig.8.

Brain (A) and brain-to-plasma concentration ratios (B) of vandetanib either alone or in the presence of everolimus and temsirolimus at 15, 30, 60 and 120min after an intravenous dose of 5mg/kg in FVB wild type mice. Results are expressed as Mean±S.E., n=3. (* represents $p<0.05$)

Table. I

Permeability values of Vandetanib across MDCK cell monolayers

		Permeability (×10^6)cm/sec		
Cell line	**Drug ± Inhibitor**	**A-B**	**B-A**	**Efflux Ratio**
MDCK-WT	Vandetanib	7.57±0.52	8.08±0.17	1.06
MDCK-MDR1	Vandetanib	5.73±0.29	4.66±0.26	0.81
MDCK-Bcrp1	Vandetanib	5.66±1.26	42.32±2.64	7.5
	Vandetanib+Ko143	8.58±0.63	8.58±0.69	1
	Vandetanib+Everolimus	7.29±1.24	10.03±0.79	1.4
	Vandetanib+Temsirolimus	10.80±1.22	11.81±0.30	1.1

Table. II

Plasma and brain pharmacokinetic parameters obtained by noncompartmental analysis of the concentration-time profile data after an i.v bolus dose of vandetanib in the absence and presence of elacridar (GF120918) in FVB wild type mice

PK parameters	vandetanib alone		vandetanib+GF120918	
	Plasma	Brain	Plasma	Brain
λ_z (h-1)	0.43	0.42	0.44	0.16
half-life (h)	1.60	1.65	1.58	4.28
Clearance(ml/min/kg)	9.36		10.33	
Volume of distribution (l/kg)	1.30		1.41	
$AUC_{(0\rightarrow tlast)}$ (μg*min/ml)	305.3 ± 12.2	62.9 ± 0.8	276.3 ±11.5	177.3 ± 18.9
$AUC_{(0\rightarrow tlast)brain}/AUC_{(0\rightarrow tlast)plasma}$	0.206		0.642	